separations

MDPI

Article

Enhanced Photocatalytic and Filtration Performance of TiO_2-Ag Composite-Coated Membrane Used for the Separation of Oil Emulsions

Ákos Ferenc Fazekas [1,2], Tamás Gyulavári [3], Áron Ágoston [4], László Janovák [4], Judit Kopniczky [5], Zsuzsanna László [1,*] and Gábor Veréb [1,*]

[1] Department of Biosystem Engineering, Faculty of Engineering, University of Szeged, Moszkvai Blvd. 9., H-6725 Szeged, Hungary; fazekas@mk.u-szeged.hu
[2] Doctoral School of Environmental Sciences, University of Szeged, Rerrich Béla Sq. 1, H-6720 Szeged, Hungary
[3] Department of Applied and Environmental Chemistry, Institute of Chemistry, University of Szeged, Rerrich Béla Sq. 1, H-6720 Szeged, Hungary; gyulavarit@chem.u-szeged.hu
[4] Department of Physical Chemistry and Materials Sciences, University of Szeged, Rerrich Béla Sq. 1, H-6720 Szeged, Hungary; agostona@chem.u-szeged.hu (Á.Á.); janovak@chem.u-szeged.hu (L.J.)
[5] Department of Optics and Quantum Electronics, Institute of Physics, University of Szeged, Dóm Sqr. 9, H-6720 Szeged, Hungary; jkopniczky@titan.physx.u-szeged.hu
* Correspondence: zsizsu@mk.u-szeged.hu (Z.L.); verebg@mk.u-szeged.hu (G.V.)

Abstract: Polyvinylidene fluoride (PVDF) membranes were coated with TiO_2 and TiO_2-Ag to enhance their efficiency for oil-in-water emulsion separation. The photocatalytic activities of the two modified membranes and their filtration performances were compared in detail. The significantly enhanced photocatalytic activity of the TiO_2-Ag composite was proved using a methyl orange (MO) solution ($c = 10^{-5}$ M) and a crude oil emulsion ($c = 50$ mg·L^{-1}). The TiO_2-Ag-coated membrane reduced the MO concentration by 87%, whereas the TiO_2-modified membrane reached only a 46% decomposition. The photocatalytic reduction in the chemical oxygen demand of the emulsion was also ~50% higher using the TiO_2-Ag-coated membrane compared to that of the TiO_2-coated membrane. The photoluminescence measurements demonstrated a reduced electron/hole recombination, achieved by the Ag nanoparticle addition (TiO_2-Ag), which also explained the enhanced photocatalytic activity. A significant improvement in the oil separation performance with the TiO_2-Ag-coated membrane was also demonstrated: a substantial increase in the flux and flux recovery ratio (up to 92.4%) was achieved, together with a notable reduction in the flux decay ratio and the irreversible filtration resistance. Furthermore, the purification efficiency was also enhanced (achieving 98.5% and 99.9% COD and turbidity reductions, respectively). Contact angle, zeta potential, scanning electron microscopy (SEM), and atomic force microscopy (AFM) measurements were carried out to explain the results. SEM and AFM images revealed that on the TiO_2-Ag-coated membrane, a less aggregated, more continuous, homogeneous, and smoother nanolayer was formed due to the ~50% more negative zeta potential of the TiO_2-Ag nanocomposite compared to that of the TiO_2. In summary, via Ag addition, a sufficiently hydrophilic, beneficially negatively charged, and homogeneous TiO_2-Ag-coated PVDF membrane surface was achieved, which resulted in the presented advantageous filtration properties beyond the photocatalytic activity enhancement.

Keywords: polyvinylidene fluoride; membrane filtration; TiO_2; silver nanoparticles; oil emulsion; zeta potential

Citation: Fazekas, Á.F.; Gyulavári, T.; Ágoston, Á.; Janovák, L.; Kopniczky, J.; László, Z.; Veréb, G. Enhanced Photocatalytic and Filtration Performance of TiO_2-Ag Composite-Coated Membrane Used for the Separation of Oil Emulsions. *Separations* **2024**, *11*, 112. https://doi.org/10.3390/separations11040112

Academic Editor: Chaolang Chen

Received: 1 March 2024
Revised: 25 March 2024
Accepted: 2 April 2024
Published: 5 April 2024

1. Introduction

As population and consumption increase, industrial production and water usage also grow significantly. Inadequate wastewater treatment can impose a considerable burden on environmental resources, such as the water supply. For instance, the water generated during oil and gas extraction amounts to over 2.5 billion cubic meters just in the United States [1]. In

addition to the petroleum industry, various other sectors also contribute to the release of oily wastewater, such as pharmaceutical, food, and metallurgical industries, and vehicle wash stations [2–4]. This type of wastewater consists of dissolved oils, emulsified oil droplets (<5–20 µm), easily removable dispersed (20–150 µm), and floating oil (>150 µm), which cannot be effectively removed through conventional treatment methods. Improperly treated oily wastewater can damage water resources and disrupt ecosystems. This is because it contains toxic compounds such as polycyclic aromatic hydrocarbons (PAHs) and heavy metals [5,6], which can bioaccumulate in living organisms and lead to biomagnification through the food chain [2,7,8]. Given the potential risks associated with these contaminants, it is essential to explore novel approaches that can effectively eliminate them.

Conventional techniques for treating oily wastewater include skimming, flotation, and sand filtration, which can eliminate floating oil with high efficiency. Moreover, chemical destabilization (coagulation/flocculation) methods are also widely used to enhance the efficiency of the previously mentioned techniques. However, for the efficient elimination of dissolved and emulsified oil droplets, advanced methods are required, such as adsorption [9], advanced oxidation processes [10], or membrane filtration [11]. These methods can be employed as a complement to conventional wastewater treatment techniques or independently to enhance treatment efficacy.

As water quality regulations tighten, membrane filtration has become popular for wastewater treatment as it can be used to demulsify and disrupt the oil–water interface in oil emulsions [12]. Membrane technology is known for its simplicity, non-chemical properties, and exceptional cleaning efficiency. However, its widespread use is hindered by rapid flux reduction, which occurs when the treated wastewater contains hydrophobic contaminants. Such wastewater leads to significant fouling of the pores, diminished lifespan, and increased energy requirement. It is necessary to develop membranes that can resist the impact of fouling and limit the interaction between pollutants and their surface.

Nowadays, an actively investigated research area of membrane separation is to improve the filtration properties of membranes by using hydrophilic and photocatalytically active nanoparticles (Al_2O_3, MgO, ZnO, SiO_2, ZrO_2, Fe_2O_3, and TiO_2) [13–18]. They cannot only reduce the pore fouling and increase the water permeability of the membranes but also potentially make them self-cleaning [19,20]. The extent of membrane fouling is primarily determined by the chemical and physical properties of the pollutants and the membrane surface. In general, low surface roughness [21], high hydrophilicity [22], and negative surface charge [23] can reduce the adhesion of oil droplets, making these properties beneficial for membranes applied for oil-in-water emulsion separation. All these factors are significantly affected by the properties of the nanomaterials used for membrane modification. Pure TiO_2, as a superhydrophilic nanomaterial, already proved to be beneficial for membrane modification [18]. However, TiO_2-based composites with higher photocatalytic activity and/or more negatively charged surfaces [13] offer further benefits. For example, carbon nanotube–TiO_2 composite-coated membranes have demonstrated increased fluxes and reduced fouling due to more negatively charged surfaces compared to solely TiO_2-coted membranes [24].

Ag deposition on TiO_2 nanoparticles is a potential solution to improve photocatalytic activity by trapping photogenerated electrons and reducing charge recombination. This has already been proven for Rhodamine B [25], tetracycline [26], sulfamethoxazole [26], metronidazole [27], oxytetracycline [28], and various endocrine disturbing compounds [29]. This effect can also be beneficial in the case of photocatalytic membranes used for the filtration of oil-in-water emulsions. Moreover, several studies show that the zeta potential of silver nanoparticles can be sufficiently negative [30–34], so the modification of TiO_2 nanoparticles with silver can potentially improve not only photocatalytic activity but filtration parameters as well. In addition, silver possesses disinfectant properties [35,36], which can be a further advantage, by preventing the formation of biofilms on membrane surfaces.

To investigate the potential advantages of TiO_2-Ag-coated membranes used in the field of crude-oil-contaminated wastewater purification (emulsion separation), we synthesized

TiO_2-Ag composites, prepared TiO_2- and TiO_2-Ag-coated polyvinylidene fluoride (PVDF) membranes and analyzed their photocatalytic activity and filtration properties. We described the photocatalytic activity not just by the degradation of widely used methyl orange (MO) but also via the photocatalytic treatment of an oil-in-water emulsion. Furthermore, to describe the cause-and-effect relationships, we carried out diffuse reflectance and photoluminescence spectroscopy measurements, including a detailed surface characterization via contact angle, zeta potential, scanning electron microscopy (SEM), and atomic force microscopy (AFM) measurements.

2. Materials and Methods

2.1. Synthesis and Characterization of the Nanoparticles

To modify the membranes, we used pure commercial Aeroxide P25 TiO_2 (Degussa-Evonik, Essen, Germany) and a silver-deposited Aeroxide P25 TiO_2 composite. The silver deposition was carried out according to the following procedure: 10 g of P25 TiO_2 was dispersed in 200 mL of MilliQ water, and 60 mL of 7.76 mM $AgNO_3$ (VWR, >99.8%) solution was added during continuous stirring. The pH was then adjusted to 7.2 using a 0.1 M NaOH solution (Sigma-Aldrich, >98%, St. Louis, MO, USA), and 80 mL of 0.242 M $NaBH_4$ (Thermo Scientific, >98%, Kandel, Germany) solution was added dropwise during continuous stirring. The beaker was covered and stirred continuously overnight to ensure the deposition of Ag nanoparticles onto the titania nanoparticles. Finally, the resulting TiO_2-Ag photocatalyst was washed via centrifugation (three times at 14,500 rpm for 3 min) using MilliQ water and dried at 70 °C. The silver content was determined to be 0.21 wt.% (Figure S1) with a HITACHI S-4700 Type II scanning electron microscope operated using its Röntec QX2 EDS detector.

The optical properties of the photocatalysts were determined via diffuse reflectance spectroscopy (DRS) between 200 and 800 nm using a CHEM 2000 UV–vis spectrometer (Ocean Optics Inc., Orlando, FL, USA). The band gap was determined by identifying the maximum of the first-order derivative of the spectrum [37]. The photoluminescence (PL) of the nanoparticles was measured with a Horiba Jobin Yvon Fluoromax-4 spectrofluorometer (Horiba Ltd., Kyoto, Japan) with an excitation wavelength of 350 nm. A band-pass filter (350 nm) was used downstream of the light source monochromator, and a high-pass filter (370 nm) was used upstream of the detector monochromator.

2.2. Modification of the Membranes with TiO_2 and TiO_2-Ag Nanomaterials

To produce the TiO_2 and TiO_2-Ag membranes, we coated commercial PVDF microfilter membranes (New Logic Research Inc., Minden, NV, USA; 0.2 µm pore diameter; ~0.0036 m^2 surface area) with physical immobilization [38]. First, 40 mg of the nanomaterial (TiO_2 or TiO_2-Ag) was suspended in 100 mL of isopropanol (c = 0.4 $g \cdot L^{-1}$), followed by ultrasonication for 1 min. Then, the homogenized suspension was immediately poured into a dead-end membrane reactor (Millipore XFUF07601, Burlington, MA, USA) and filtered through the membrane at a pressure of 0.3 MPa. The as-prepared membranes were left to dry at room temperature for two days before application.

2.3. Production of Oil Emulsions and Filtration Experiments

To produce the oil emulsions used for the filtration experiments, first, we thoroughly blended 1 wt.% crude oil (provided by MOL Zrt, Algyő, Hungary) with ultrapure water at 35,000 rpm for 1 min using a mixer (Einhell TC-MG 135 E, Landau an der Isar, Germany). Then, 20 mL of the as-prepared oil dispersion was added into 480 mL of ultrapure water and homogenized for 10 min with an immersion-type ultrasonicator (Hielscher UP200S, Teltow, Germany) to create stable oil-in-water emulsions. The main parameters of the prepared oil emulsions are given in Table 1.

Table 1. Main parameters of the oil emulsion used for filtration experiments.

COD ($mg \cdot L^{-1}$)	Turbidity (NTU)	TOG/TPH ($mg \cdot L^{-1}$)	pH	Zeta Potential (mV)	Average Oil Droplet Size (nm)
549 ± 12	280 ± 9	108 ± 2.5	6.2 ± 0.1	−43.3 ± 7.1	587

To filter the crude oil emulsions (V = 250 mL), we placed the membranes (active filtration area = 36.2 cm^2) in the same membrane reactor (Millipore XFUF07601, Burlington, MA, USA), and the process was carried out at a transmembrane pressure of 0.1 MPa up to a volume reduction ratio (VRR) of five (until producing 200 mL of permeate) at a constant stirring rate of 350 rpm.

We evaluated the purification efficiency of the membranes via turbidity and chemical oxygen demand (COD) measurements. For this purpose, we used the standard potassium dichromate oxidation method. The experiments were preceded by digestion at 150 °C for 120 min; then, standard test tubes were used (Hanna Instruments, Woonsocket, RI, USA). We measured the turbidity values with a nephelometric turbidity meter (Hach 2100 N, Loveland, CO, USA). The values are expressed as "NTU" (nephelometric turbidity units). We calculated the purification efficiencies (R) based on Equation (1):

$$R = \left(1 - \frac{C}{C_0}\right) \times 100\% \quad (1)$$

During the measurements, we recorded the flux (J) continuously by following the permeate weight and using Equation (2):

$$J = \frac{dV}{A_m \times dt} \ \left(\frac{L}{m^2 \times h}\right) \quad (2)$$

where dt is the time (h) at which the permeate weight was measured, A_m is the active filtration area of the membrane we applied (m^2), J is the flux, and dV is the permeate volume (L).

We investigated the fouling properties of the membranes via the resistance-in-series model [39,40]. The own resistance of the membranes (R_m) and the irreversible (R_{irrev}), re-versible (R_{rev}), and total (R_{total}) filtration resistances were calculated using the following equations:

$$R_m = \frac{\Delta p}{J_w \times \eta_w} \ (m^{-1}) \quad (3)$$

$$R_{irrev} = \frac{\Delta p}{J_{ww} \times \eta_w} - R_m \ (m^{-1}) \quad (4)$$

$$R_{rev} = \frac{\Delta p}{J_c \times \eta_{ww}} - R_{irrev} - R_m \ (m^{-1}) \quad (5)$$

$$R_{total} = R_m + R_{rev} + R_{irrev} (m^{-1}) \quad (6)$$

where Δp is the transmembrane pressure we applied (0.1 MPa), J_w is the flux of the water defined by the clean membrane, η_w is the water viscosity at 25 °C (Pa·s), J_{ww} is the flux of the water measured following the filtration of oil and the purification of the membranes we used (by rinsing vigorously with ultrapure water), J_c is the steady-state flux measured at the end of the filtrations experiments (VRR = 5), and η_{ww} is the viscosity of the wastewater (that is, the used oil-in-water emulsion).

As the next step, we calculated the flux recovery ratio (FRR). FRR shows the degree of the initial water flux that can be recovered by rinsing the membrane after its application (that is, after filtering oil emulsions). FRR can be determined based on Equation (7):

$$FRR = \frac{J_{wA}}{J_w} \times 100 \ (\%) \quad (7)$$

where J_w is the pure water flux of the membrane measured prior to its utilization for filtering oil emulsions, and J_{wA} is the pure water flux after filtering and cleaning the surface of the membrane surface.

By comparing the flux value measured at the end of filtration experiments (J_c) to the clean water flux measured with ultrapure water before filtering oil emulsions (J_w), we can obtain the flux decay ratio (FDR) as follows:

$$FDR = \frac{J_w - J_c}{J_w} \times 100\ (\%) \quad (8)$$

2.4. Characterization of the Membrane Surface

The morphology of the membrane surfaces was investigated by SEM (Hitachi S-4700 Type II) using an acceleration voltage of 10 kV.

AFM was used to characterize the surface roughness of the coated membranes using a PSIA XE-100 type device (South Korea; NC-AFM head mode).

Membrane surfaces were also characterized by zeta potential measurements. For this purpose, we employed a streaming potential technique and an Anton Paar SurPASS 3 instrument (AntonPaar Gmbh, Graz, Austria). The measurement was carried out using an adjustable gap cell and two membrane pieces (10 mm × 20 mm) fixed via double-sided adhesive tapes. The pH range we used was ~2–8 (c_{KCl} = 0.001 mol·L^{-1}), which was set by KOH and HCl solutions. The pH values were continuously recorded with a pH electrode.

Wetting properties of both modified and unmodified membranes were investigated by contact angle measurements with a Dataphysics Contact Angle System OCA15Pro (Filderstadt, Germany) device. For this purpose, a Hamilton pipette was used to precisely dispense 10 µL of ultrapure water onto the membrane surfaces. Then, the contact angles were recorded within 1 s between the water droplets and the membrane. The measurements were repeated three times, and the average values were considered.

2.5. Photocatalytic Experiments

The photocatalytic activities of the modified membranes were measured via the photocatalytic oxidation of 300 mL of a methyl orange solution (c = 10^{-5} M) or an oil-in-water emulsion (c = 50 mg·L^{-1}) in a double-walled glass photoreactor (Figure 1) at 20 °C.

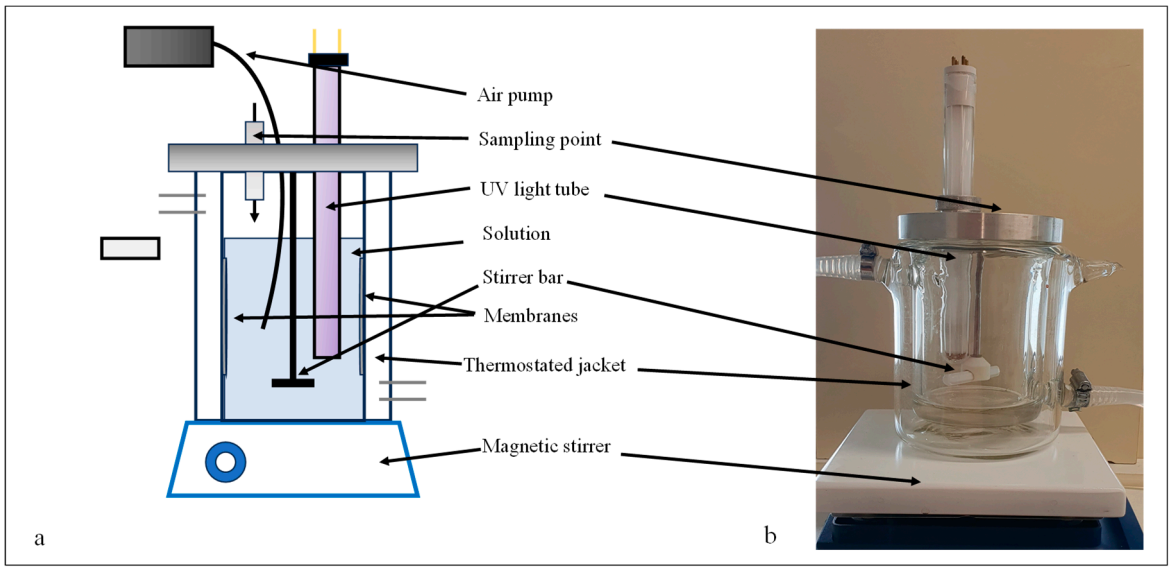

Figure 1. Schematic figure (**a**) and photograph of the photocatalytic reactor (**b**) used for measuring the photocatalytic activities of the membranes.

The photocatalytic degradations were carried out at a continuous stirring rate of 250 rpm. The light source was a UV lamp (P = 10 W, λ_{max} = 360 nm, Lighttech, Dunakeszi,

Hungary) immersed into the reactor, while two membranes were fixed on the inner wall of the photoreactor. The methyl orange decompositions were carried out for 4 h, preceded by 1 h of adsorption. Samples were taken every 20 min, and changes in absorbance values were monitored with a UV–vis spectrophotometer (Biowave WPA II) at 466 nm. The photocatalytic degradation of oil emulsions was conducted for 8 h, samples were taken every 2 h, and finally, the COD values were measured (Hanna Instruments, Woonsocket, RI, USA).

3. Results

3.1. Photocatalytic Activity of the Modified Membranes

To the best of our knowledge, the photocatalytic activity of silver-deposited titanium dioxide-coated membranes has not been demonstrated for oil emulsions before. Therefore, in this work, the photocatalytic degradations of methyl orange solutions and oil emulsions were examined (Figure 2).

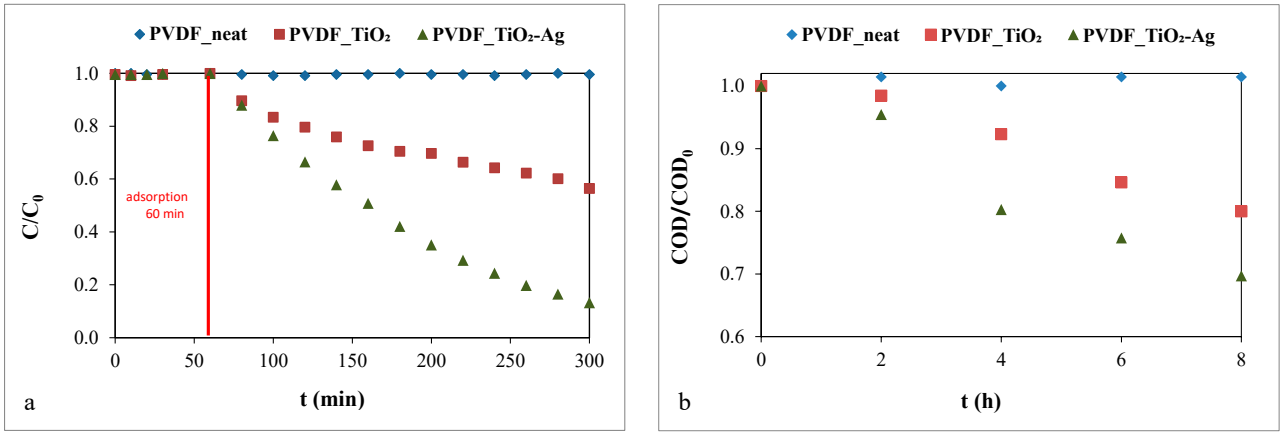

Figure 2. Photocatalytic degradation of (**a**) the methyl orange solution (c = 10^{-5} M) and (**b**) the oil emulsion (c = 50 mg·L^{-1}).

No photocatalytic degradation was measured for the neat PVDF membrane, as expected. However, the modified membranes proved to be photocatalytically active, as both the dye concentration and the COD of the oil emulsion decreased significantly. Regarding the methyl orange solution (Figure 2a), the presence of silver on the TiO_2 nanoparticles outstandingly improved the photocatalytic activity, reaching a decomposition of 87%. In comparison, the TiO_2-modified membrane demonstrated only 46% decomposition after 240 min of irradiation. The increased photocatalytic activity of the silver-deposited TiO_2 was also proved for oil emulsion decomposition. The COD reduction was ~1.5 times higher compared to that of the pure TiO_2-coated membrane: the COD of the initial oil emulsion was reduced by ~30% with the TiO_2-Ag-coated membranes during the 8 h of photodegradation, while the reduction was ~20% when the pure TiO_2-coated membrane was applied. To give some explanation for the significant difference in the photocatalytic activities of TiO_2 and TiO_2-Ag photocatalysts, we performed DRS and PL measurements.

The light absorption properties of the samples were measured by DRS (Figure 3a), and the first-order derivatives of the reflectance values as a function of wavelength are shown in Figure 3b. Figure 3a shows that the silver-deposited titania absorbs a significant number of photons in the visible light range, especially around 550 nm, in accordance with the slightly purplish color of this composite. However, this does not necessarily mean that it can be excited by those absorbed photons. Based on the first-order derivate DR spectra in Figure 3b, which provide reliable information about the excitability of photocatalysts [37], there is no significant difference in the band gap values of these titania, so the deposited silver did not extend the excitability range of the TiO_2.

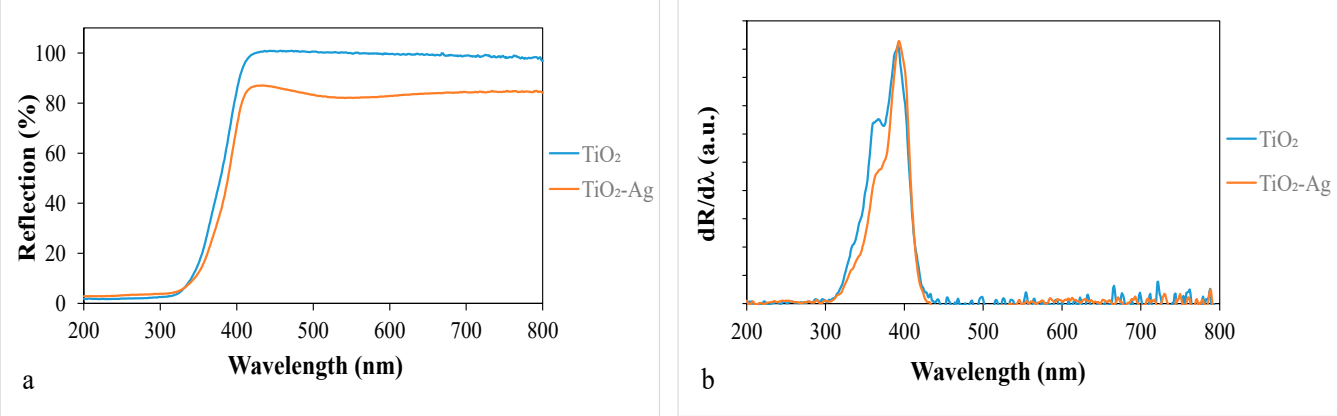

Figure 3. (**a**) Diffuse reflectance spectra of the nanomaterials and (**b**) their first-order derivatives.

The PL spectra of the samples provide important information about the recombination of photogenerated charge carriers. The variation in the emission intensity (Figure 4) shows the extent of recombination by photon emission relative to each other [41]. The emission intensity of the TiO_2-Ag sample is reduced compared to that of TiO_2, which means that recombination by photon emission is lower in TiO_2-Ag than in TiO_2. Since fewer excitons (electron/hole pairs) recombine, the electrons are involved in useful processes such as the direct oxidation of contaminants and/or the production of oxidative free radicals. These findings are supported by the literature, according to which the silver deposited on the surface of TiO_2 serves as a location where electrons accumulate [42].

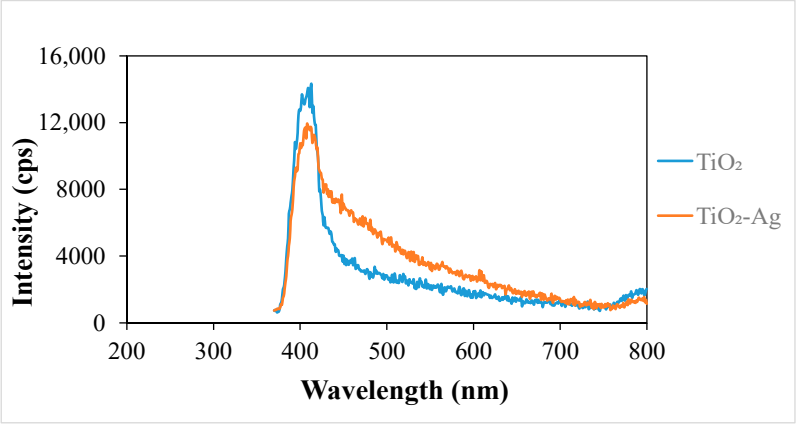

Figure 4. Photoluminescence spectra of the nanomaterials.

3.2. Filtration of the Oil-in-Water Emulsions with the Different Membranes

The filtration parameters and key characteristics of the commercial (unmodified) PVDF membranes and the TiO_2- and TiO_2-Ag-coated membranes are summarized in Table 2. Additionally, the calculated filtration resistance values are illustrated in Figure 5.

Table 2. Membrane filtration parameters and the main surface properties of the membranes.

Membranes	Contact Angles (°)	J_{before} (L m^{-2} h^{-1})	$J_{effluent}$ (L m^{-2} h^{-1})	J_{after} (L m^{-2} h^{-1})	FRR (%)	FDR (%)	Turbidity Reduction (%)	COD Reduction (%)	Zeta Potential at pH~6 (mV)
PVDF_neat	46.6 ± 0.9	5638	24	2567	45.5	99.6	97.3	94.4	−11 ± 0.7
PVDF_TiO_2	0 ± 0.3	3608	37	2572	71.3	99	99	96.4	−25 ± 3.4
PVDF_TiO_2-Ag	13.5 ± 0.7	2285	83	2112	92.4	96.4	99.9	98.5	−37.6 ± 1.6

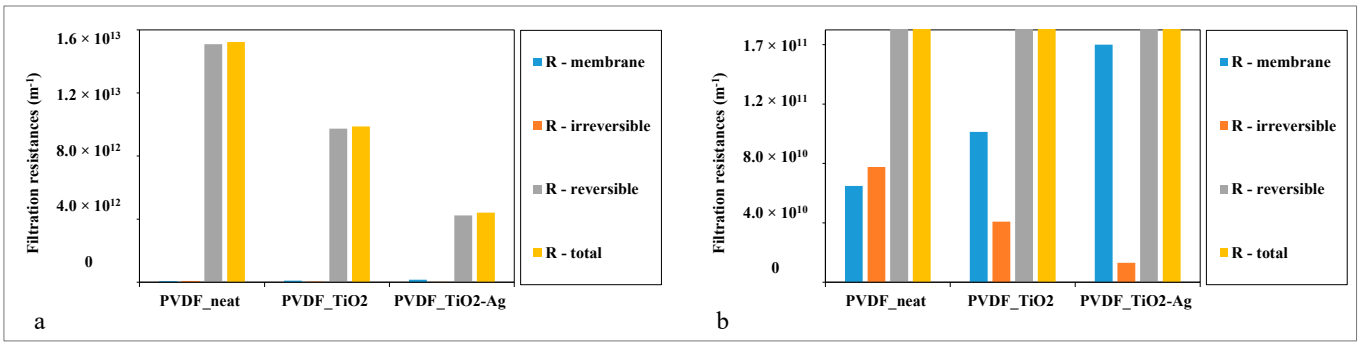

Figure 5. Filtration resistances of the neat, TiO_2-, and TiO_2-Ag-coated membranes (**a**) for comparing the reversible and the total filtration resistances and (**b**) for comparing the membrane resistances and the irreversible filtration resistances after magnification.

Membrane hydrophilicity is a crucial parameter in oil/water separation that affects the filtration parameters significantly, as higher hydrophilicity (lower water contact angle) reduces the adhesion ability of the hydrophobic oil droplets. As expected, both surface modifications effectively reduced the water contact angles on the membranes compared to the uncoated (PVDF-Neat) membrane (contact angle: 46.6 ± 0.9°). Coating with TiO_2 nanoparticles resulted in a superhydrophilic surface (contact angle: 0 ± 0.3°), while after coating with the TiO_2-Ag composite, a slightly higher value was obtained (contact angle: 13.5 ± 0.7°). This can be attributed to the hydrophobic nature of AgO [43–45], which can form on the surface of the deposited silver. Table 2 demonstrates that the pure water fluxes of the modified membranes are significantly lower compared to those of the neat membrane (5638, 3608, and 2285 L m^{-2} h^{-1} for the neat, TiO_2-coated, and TiO_2-Ag-coated membranes, respectively). This is a natural consequence of the additional nanoparticle layer on the surface. The water flux of the TiO_2-Ag-coated membrane is ~37% lower than that of the TiO_2-coated membrane, even though its hydrophilicity is only slightly lower (Table 2). This means that the pure TiO_2 layer allows easier water penetration compared to the TiO_2-Ag layer. This statement is in good accordance with the higher hydrophilicity of the pure TiO_2 coating, but the significant difference suggests further affecting factors that will be discussed later. Based on the flux values measured at the end of the filtration experiments (at VRR = 5), it can be inferred that the surface modification with TiO_2 resulted in a flux improvement of ~54%, while the modification with the TiO_2-Ag composite provided a much more significant improvement of ~246%. Additionally, the FRRs also showed significant improvement, as the 45.5% value of the neat membrane increased to 71.3% and 92.4% in the case of the TiO_2-coated and the TiO_2-Ag-coated membranes, respectively.

For a more detailed discussion, the filtration resistances were also calculated and are demonstrated in Figure 5.

In accordance with the flux enhancements, Figure 5a demonstrates a significant reduction in the total and reversible filtration resistances achieved by the TiO_2 and TiO_2-Ag surface modifications. Even though the resistance of the neat PVDF membrane was increased by the coating layers, the irreversible filtration resistance was significantly reduced (Figure 5b). Irreversible resistance is the resistance that is caused by contaminants that cannot be removed by simple water flushing, which also provides information about the fouling of the membrane. The reduction in this resistance can lead to the improved lifetime and cleanability of the membranes, especially in the case of the TiO_2-Ag composite coating.

The TiO_2-Ag coating was also the most advantageous regarding the purification efficiencies of the filtration experiments (the calculated values are given in Table 2). Even the unmodified membrane ensured good purification efficiency with 94% and 97% COD and turbidity reductions, respectively. For the TiO_2-Ag-coated membrane, these values were 98.5% and 99.9%, respectively, which are even higher than the values obtained for the pure TiO_2-coated membrane.

The advantageous effects conveyed by the TiO_2-Ag coating (higher flux of the oil emulsion, lower total and irreversible filtration resistances, and higher purification efficiency) are in good accordance with its sufficiently high hydrophilicity and the relatively higher zeta potential (compared to the TiO_2 coating; Table 2). However, the relatively high membrane resistance and the relatively low water flux of the TiO_2-Ag-modified membrane suggest some significant morphological differences between the pure TiO_2- and the TiO_2-Ag-composite-coated membranes. According to the DVLO theory, the uniformity of particles (titania particles in our case) in suspensions is affected by the balance between the attractive and repulsive forces that exist between them. The zeta potential of the particles functions as a repulsive force, resulting in electrostatic stabilization [46,47]. Therefore, the differences in the zeta potential of the two titania (Table 2) could alter the morphology of the nanolayers of the membranes. This hypothesis is supported by the SEM images of the membrane surfaces presented in Figure 6 and by the AFM images in Figure 7 as well.

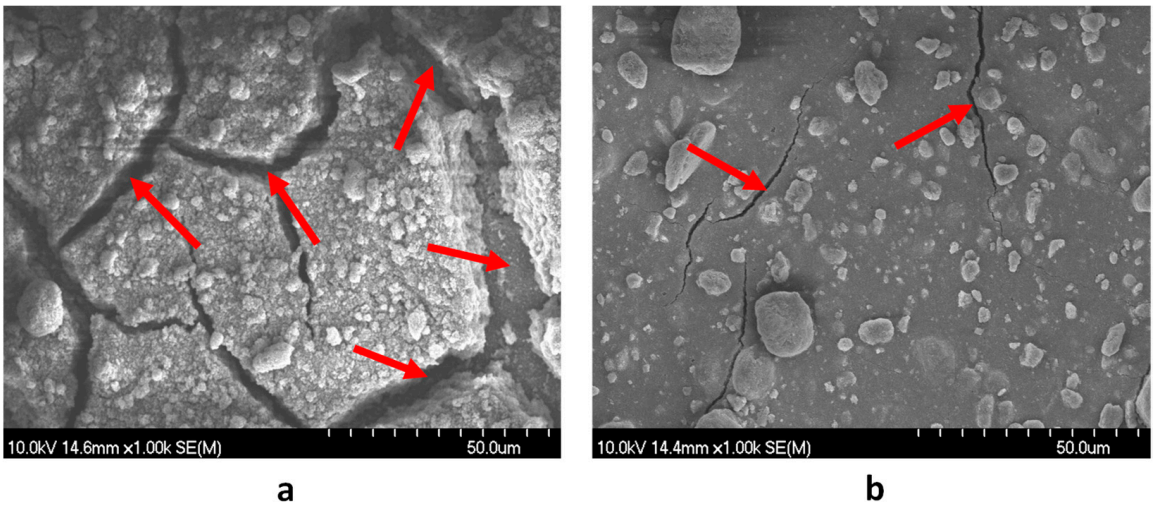

Figure 6. SEM micrographs of the (**a**) TiO_2- and (**b**) TiO_2-Ag-coated membranes. The red arrows indicate the difference in the continuity/homogeneity of membrane coatings.

The nanoparticle layer on the TiO_2-modified membranes consists of large aggregates and does not form a continuous, homogeneous layer (Figure 6a). In contrast, when the surface was modified with TiO_2-Ag, a less significant aggregation of the nanoparticles was observed (Figure 6b). AFM images (Figure 7) also show big aggregates and a rougher surface for the TiO_2-coated membrane compared to the much smoother surface of the TiO_2-Ag-coated membrane. These results are in good accordance with the zeta potential values (Table 2) of the TiO_2 and TiO_2-Ag-coated membrane surfaces, as the latter was ~50% more negative (-37.6 ± 1.6 mV) than the former (-25 ± 3.4 mV). Moreover, based on the literature, the nanoparticles can form stable and homogeneous suspensions when the surface charge is above +30 mV or below -30 mV [46,47]. This can explain the significant differences in the homogeneity of the nanolayers, as their zeta potentials are above (for TiO_2) and below (for TiO_2-Ag) this crucial -30 mV value. The resulting more homogeneous and compact TiO_2-Ag composite layer explains the significantly lower pure water flux and higher membrane resistance of the TiO_2-Ag-coated membrane compared to the TiO_2-coated membrane. These properties, together with the reduced surface roughness, could also contribute to the significantly higher emulsion fluxes and purification efficiencies. Moreover, the negative zeta potential of the TiO_2-Ag-coated membrane was beneficial concerning the electrostatic repulsive forces between the membrane and the negatively charged oil droplets. Thus, their ability to attach to the surface was reduced, contributing to the measured higher flux and flux recovery ratio and the reduced irreversible resistance.

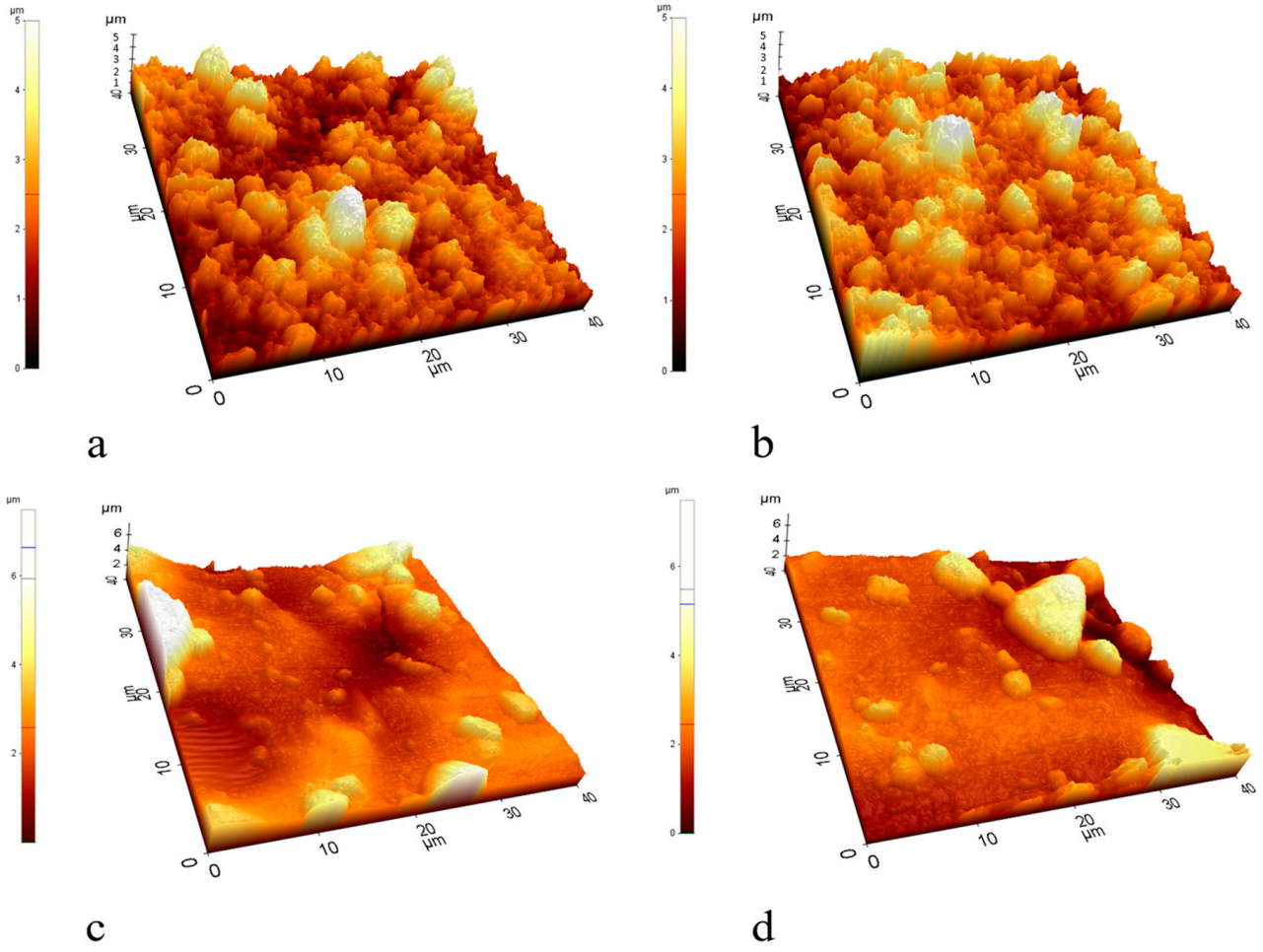

Figure 7. AFM images of the (**a**,**b**) TiO_2- and (**c**,**d**) TiO_2-Ag-coated membranes.

3.3. Comparison of the Main Separation Results with Other Relevant Studies

For comparison, Table 3 demonstrates a comprehensive summary of the main parameters of other studies, which also used TiO_2-Ag- (or Ag-) modified membranes for the separation of different kinds of oil emulsions. It should be noted that the membrane modification techniques and the types/concentrations of oil emulsions used in these studies differ from those used in our study. Despite this, in general, the results of these studies also indicate that the utilization of Ag nanoparticles for membrane modification usually significantly improved the filtration properties, reduced the fouling rate, and yielded retention values similar to the results presented in our work (>98.5%). For instance, R. Torres Mendiate et al. [48] modified PVDF membranes with silver nanoparticles and achieved a fourfold increase in the flux value (12 and 45 L m^{-2} h^{-1} were measured for the unmodified and modified membranes, respectively) in the case of a vegetable oil-containing emulsion. This result is consistent with our flux increase (24 and 83 L m^{-2} h^{-1} for the unmodified and modified membranes, respectively).

Table 3. Comparison of the main parameters and results with other relevant studies, applying TiO_2-Ag- or Ag- modified membranes for the separation of oil emulsions.

	Membrane or Underlayer	Modifier Nanomaterial	Type of Oil (Concentration)	Pressure	Surfactants (Concentration)	Water Flux (L m^{-2} h^{-1})	Effluent Flux (L m^{-2} h^{-1})	Rejection (%)	Fouling Indicators
[48]	PVDF	Ag	vegetable oil (w/w = 1/1 o:w)	0.002 MPa	Triton X100	unmodified: -modified: -	unmodified: ~12 modified: ~45	>96	unmodified: 22.4 (FRR) modified: 38.1 (FRR)—after ten runs
[49]	CA	RGO-Ag-TiO_2	n.a. (v/v = 1/100 o:w)	0.09 MPa (vacuum)	SDS (0.4 g·L^{-1})	unmodified: 20,472 modified: 191	~30	>97	no obvious decline after six cycled experiments
[50]	Copper mesh	TiO_2-SGO-Ag	gasoline, n-heptane (v/v = 1/10 o:w)	gravity	CTAB (0.5 g·L^{-1})	-	~50	>99	no obvious decline after ten cycled experiments
[51]	Ceramic (TiO_2/ZrO_2)	Ag-CuO	gasoline (1000 ppm)	0.1 MPa (vacuum)	Tween-20 (0.5 g·L^{-1})	unmodified: ~230 modified: ~300	unmodified: ~130 modified: ~220	>97	unmodified: 77.19 (FRR) modified: 90.62 (FRR)
Current study	PVDF	TiO_2-Ag	crude oil (400 ppm)	0.1 MP	-	unmodified: 5638 modified: 2285	unmodified: 24 modified: 83	>98.5	unmodified: 45.5 (FRR) modified: 92.4 (FRR)

4. Conclusions

To the best of our knowledge, this study describes first in detail the reasons behind the beneficial properties of silver-containing titanium dioxide as a membrane surface modifier for both the photocatalytic degradation and membrane separation of crude oil-contaminated wastewater (emulsion).

Applying TiO_2-Ag nanocomposite on the membrane surface significantly improved the photocatalytic decomposition of the oil emulsion, as the COD reduction was ~1.5 times higher compared to the pure TiO_2-coated membrane. The first-order derivatives of the DR spectra did not demonstrate significant differences in the bandgap values of the two titania. However, the PL spectra indicated that recombination by photon emission was suppressed in the TiO_2-Ag composite (compared to pure TiO_2), which explained the enhanced photocatalytic activity.

Surface modification with the TiO_2 resulted in a flux improvement of ~54%, while modification with the TiO_2-Ag composite provided a much higher enhancement of ~246%. The FRRs also showed a significant improvement, as the 45.5% value of the neat membrane increased to 71.3% and 92.4% for the TiO_2-coated and the TiO_2-Ag-coated membranes, respectively. In accordance with the flux enhancements, a significant reduction in both the total and reversible filtration resistances was achieved by TiO_2 and TiO_2-Ag surface modifications. Moreover, the irreversible filtration resistance was also reduced, especially for the TiO_2-Ag composite coating, improving the lifetime and cleanability of the membranes. Coating with TiO_2-Ag was also the most advantageous regarding the purification efficiencies of the emulsion filtrations.

All these advantageous effects of TiO_2-Ag coating directly originate from its sufficiently high hydrophilicity and relatively high zeta potential. The latter also resulted in a smoother, more continuous, and homogeneous coating compared to the one obtained for the pure TiO_2-coated membranes, which also contributed to the beneficial filtration properties.

Based on the presented results, TiO_2-Ag nanocomposites are promising for modifying membranes used for the filtration of oily wastewater. Therefore, this composite is worth investigating further in future studies aiming to develop nanocomposite membranes produced by either grafting and/or blending methods, which are durable enough for long-term (practical) utilization as well.

Supplementary Materials: The following supporting information can be downloaded at: https://www.mdpi.com/article/10.3390/separations11040112/s1, Figure S1: Elemental analysis of the TiO_2-Ag-coated PVDF membrane.

Author Contributions: Conceptualization, G.V. and Z.L.; methodology, Á.F.F., T.G., L.J., J.K. and Á.Á.; software, Á.F.F., T.G. and G.V.; investigation, Á.F.F., J.K. and Á.Á.; writing—original draft preparation, Á.F.F., T.G., Á.Á. and G.V.; writing—review and editing, Á.F.F., T.G., L.J., J.K., Z.L. and G.V.; visualization, Á.F.F.; supervision, G.V., L.J. and Z.L.; funding acquisition, G.V. All authors have read and agreed to the published version of the manuscript.

Funding: This research was funded by the Hungarian National Research, Development and Innovation Office—NKFIH in the framework of the "Development and application of nanoparticle modified membranes for the efficient treatment of oil-contaminated waters" project (NKFI_FK_20_135202).

Data Availability Statement: Data are contained within the article and supplementary materials.

Acknowledgments: The authors are thankful for the financial support provided by the Hungarian National Research, Development and Innovation Office—NKFIH (FK_20_135202). The authors are grateful to Tünde Baló for the administrative work.

Conflicts of Interest: The authors declare no conflicts of interest. The funders had no role in the design of the study; in the collection, analyses, or interpretation of data; in the writing of the manuscript; or in the decision to publish the results.

References

1. Kasemset, S.; Lee, A.; Miller, D.J.; Freeman, B.D.; Sharma, M.M. Effect of Polydopamine Deposition Conditions on Fouling Resistance, Physical Properties, and Permeation Properties of Reverse Osmosis Membranes in Oil/Water Separation. *J. Membr. Sci.* **2013**, *425–426*, 208–216. [CrossRef]
2. Zhao, C.; Zhou, J.; Yan, Y.; Yang, L.; Xing, G.; Li, H.; Wu, P.; Wang, M.; Zheng, H. Application of Coagulation/Flocculation in Oily Wastewater Treatment: A Review. *Sci. Total Environ.* **2021**, *765*, 142795. [CrossRef]
3. Abuhasel, K.; Kchaou, M.; Alquraish, M.; Munusamy, Y.; Jeng, Y.T. Oily Wastewater Treatment: Overview of Conventional and Modern Methods, Challenges, and Future Opportunities. *Water* **2021**, *13*, 980. [CrossRef]
4. Putatunda, S.; Bhattacharya, S.; Sen, D.; Bhattacharjee, C. A Review on the Application of Different Treatment Processes for Emulsified Oily Wastewater. *Int. J. Environ. Sci. Technol.* **2018**, *16*, 2525–2536. [CrossRef]
5. Kundu, P.; Mishra, I.M. Treatment and Reclamation of Hydrocarbon-Bearing Oily Wastewater as a Hazardous Pollutant by Different Processes and Technologies: A State-of-the-Art Review. *Rev. Chem. Eng.* **2018**, *35*, 73–108. [CrossRef]
6. Radelyuk, I.; Tussupova, K.; Zhapargazinova, K. *Impact of Oily Wastewater for Public Health in Rural Area: A Case Study of Kazakhstan*; Copernicus GmbH: Göttingen, Germany, 2020.
7. Meneceur, S.; Bouafia, A.; Laouini, S.E.; Mohammed, H.A.; Daoudi, H.; Chami, S.; Hasan, G.G.; Abdullah, J.A.A.; Salmi, C. Removal Efficiency of Heavy Metals, Oily in Water, Total Suspended Solids, and Chemical Oxygen Demand from Industrial Petroleum Wastewater by Modern Green Nanocomposite Methods. *J. Environ. Chem. Eng.* **2023**, *11*, 111209. [CrossRef]
8. Nascimento, B.Z.; Muniz, E.P.; Bueno Cotta, A.J.; Couto Oliveira, F.D.; Sérgio da Silva Porto, P. Oily Wastewater Treatment by a Continuous Flow Electrocoagulation Reactor with Polarity Switch: Assessment of the Relation between Process Variables and the Aluminum Released to the Environment. *J. Environ. Manag.* **2023**, *347*, 119072. [CrossRef] [PubMed]
9. Teow, Y.H.; Isma Nordin, P.M.; Ahmad Juanda, N.I.; Mohd Shafi, M.A.; Krishnan, P. A Review on Adsorption Process for the Treatment of Oily Wastewater. *Adv. Environ. Eng. Res.* **2023**, *4*, 016. [CrossRef]
10. Elmobarak, W.F.; Hameed, B.H.; Almomani, F.; Abdullah, A.Z. A Review on the Treatment of Petroleum Refinery Wastewater Using Advanced Oxidation Processes. *Catalysts* **2021**, *11*, 782. [CrossRef]
11. Yalcinkaya, F.; Boyraz, E.; Maryska, J.; Kucerova, K. A Review on Membrane Technology and Chemical Surface Modification for the Oily Wastewater Treatment. *Materials* **2020**, *13*, 493. [CrossRef]
12. Hong, J.; Wang, Z.; Li, J.; Xu, Y.; Xin, H. Effect of Interface Structure and Behavior on the Fluid Flow Characteristics and Phase Interaction in the Petroleum Industry: State of the Art Review and Outlook. *Energy Fuels* **2023**, *37*, 9914–9937. [CrossRef]
13. Ni, P.; Zeng, J.; Chen, H.; Yang, F.; Yi, X. Effect of Different Factors on Treatment of Oily Wastewater by TiO_2/Al_2O_3-PVDF Ultrafiltration Membrane. *Environ. Technol.* **2021**, *43*, 2981–2989. [CrossRef]
14. Zhou, J.; Xia, Y.; Gong, Y.; Li, W.; Li, Z. Efficient Natural Organic Matter Removal from Water Using Nano-MgO Coupled with Microfiltration Membrane Separation. *Sci. Total Environ.* **2020**, *711*, 135120. [CrossRef] [PubMed]
15. Kusworo, T.D.; Kumoro, A.C.; Aryanti, N.; Utomo, D.P. Removal of Organic Pollutants from Rubber Wastewater Using Hydrophilic Nanocomposite rGO-ZnO/PES Hybrid Membranes. *J. Environ. Chem. Eng.* **2021**, *9*, 106421. [CrossRef]
16. Alkindy, M.B.; Naddeo, V.; Banat, F.; Hasan, S.W. Synthesis of Polyethersulfone (PES)/GO-SiO_2 Mixed Matrix Membranes for Oily Wastewater Treatment. *Water Sci. Technol.* **2019**, *81*, 1354–1364. [CrossRef]
17. Wang, X.; Sun, K.; Zhang, G.; Yang, F.; Lin, S.; Dong, Y. Robust Zirconia Ceramic Membrane with Exceptional Performance for Purifying Nano-Emulsion Oily Wastewater. *Water Res.* **2022**, *208*, 117859. [CrossRef]
18. Tetteh, E.K.; Rathilal, S.; Asante-Sackey, D.; Chollom, M.N. Prospects of Synthesized Magnetic TiO_2-Based Membranes for Wastewater Treatment: A Review. *Materials* **2021**, *14*, 3524. [CrossRef]
19. Sagir, M.; Tahir, M.B.; Akram, J.; Tahir, M.S.; Waheed, U. Nanoparticles and Significance of Photocatalytic Nanoparticles in Wastewater Treatment: A Review. *Curr. Anal. Chem.* **2020**, *17*, 38–48. [CrossRef]
20. Nascimbén Santos, É.; László, Z.; Hodúr, C.; Arthanareeswaran, G.; Veréb, G. Photocatalytic Membrane Filtration and Its Advantages over Conventional Approaches in the Treatment of Oily Wastewater: A Review. *Asia-Pac. J. Chem. Eng.* **2020**, *15*, e2533. [CrossRef]
21. Panda, S.R.; Bhandaru, N.; Mukherjee, R.; De, S. Ultrafiltration of Oily Waste Water: Contribution of Surface Roughness in Membrane Properties and Fouling Characteristics of Polyacrylonitrile Membranes. *Can. J. Chem. Eng.* **2015**, *93*, 2031–2042. [CrossRef]
22. Shahruddin, M.Z.; Zakaria, N.; Diana Junaidi, N.F.; Alias, N.H.; Othman, N.H. Study of the Effectiveness of Titanium Dioxide (TiO_2) Nanoparticle in Polyethersulfone (PES) Composite Membrane for Removal of Oil in Oily Wastewater. *J. Appl. Membr. Sci. Amp; Technol.* **2017**, *19*, 33–42. [CrossRef]
23. Lin, A.; Shao, S.; Li, H.; Yang, D.; Kong, Y. Preparation and Characterization of a New Negatively Charged Polytetrafluoroethylene Membrane for Treating Oilfield Wastewater. *J. Membr. Sci.* **2011**, *371*, 286–292. [CrossRef]
24. Fekete, L.; Fazekas, Á.F.; Hodúr, C.; László, Z.; Ágoston, Á.; Janovák, L.; Gyulavári, T.; Pap, Z.; Hernadi, K.; Veréb, G. Outstanding Separation Performance of Oil-in-Water Emulsions with TiO_2/CNT Nanocomposite-Modified PVDF Membranes. *Membranes* **2023**, *13*, 209. [CrossRef] [PubMed]
25. Albiter, E.; Valenzuela, M.A.; Alfaro, S.; Valverde-Aguilar, G.; Martínez-Pallares, F.M. Photocatalytic Deposition of Ag Nanoparticles on TiO_2: Metal Precursor Effect on the Structural and Photoactivity Properties. *J. Saudi Chem. Soc.* **2015**, *19*, 563–573. [CrossRef]

26. Tiwari, A.; Shukla, A.; Lalliansanga; Tiwari, D.; Lee, S.M. Nanocomposite Thin Films Ag0(NP)/TiO_2 in the Efficient Removal of Micro-Pollutants from Aqueous Solutions: A Case Study of Tetracycline and Sulfamethoxazole Removal. *J. Environ. Manag.* **2018**, *220*, 96–108. [CrossRef] [PubMed]
27. Aoudjit, L.; Salazar, H.; Zioui, D.; Sebti, A.; Martins, P.M.; Lanceros-Mendez, S. Reusable Ag@TiO_2-Based Photocatalytic Nanocomposite Membranes for Solar Degradation of Contaminants of Emerging Concern. *Polymers* **2021**, *13*, 3718. [CrossRef] [PubMed]
28. Ibrahim, I.; Belessiotis, G.V.; Antoniadou, M.; Kaltzoglou, A.; Sakellis, E.; Katsaros, F.; Sygellou, L.; Arfanis, M.K.; Salama, T.M.; Falaras, P. Silver Decorated TiO_2/g-C3N4 Bifunctional Nanocomposites for Photocatalytic Elimination of Water Pollutants under UV and Artificial Solar Light. *Results Eng.* **2022**, *14*, 100470. [CrossRef]
29. Leong, K.H.; Gan, B.L.; Ibrahim, S.; Saravanan, P. Synthesis of Surface Plasmon Resonance (SPR) Triggered Ag/TiO_2 Photocatalyst for Degradation of Endocrine Disturbing Compounds. *Appl. Surf. Sci.* **2014**, *319*, 128–135. [CrossRef]
30. Hedberg, J.; Lundin, M.; Lowe, T.; Blomberg, E.; Wold, S.; Wallinder, I.O. Interactions between Surfactants and Silver Nanoparticles of Varying Charge. *J. Colloid Interface Sci.* **2012**, *369*, 193–201. [CrossRef]
31. Sujatha, V.; Kaviyasri, G.; Venkatesan, A.; Thirunavukkarasu, C.; Acharya, S.; Bin Dayel, S.; Al-Ghamdi, S.; Hassan Abdelzaher, M.; Shahid, M.; Ramesh, T. Biomimetic Formation of Silver Oxide Nanoparticles through Diospyros Montana Bark Extract: Its Application in Dye Degradation, Antibacterial and Anticancer Effect in Human Hepatocellular Carcinoma Cells. *J. King Saud Univ. Sci.* **2023**, *35*, 102563. [CrossRef]
32. Chinni, S.V.; Gopinath, S.C.B.; Anbu, P.; Fuloria, N.K.; Fuloria, S.; Mariappan, P.; Krusnamurthy, K.; Veeranjaneya Reddy, L.; Ramachawolran, G.; Sreeramanan, S.; et al. Characterization and Antibacterial Response of Silver Nanoparticles Biosynthesized Using an Ethanolic Extract of Coccinia Indica Leaves. *Crystals* **2021**, *11*, 97. [CrossRef]
33. Lopez-Carrizales, M.; Pérez-Díaz, M.A.; Mendoza-Mendoza, E.; Peralta-Rodríguez, R.D.; Ojeda-Galván, H.J.; Portales-Pérez, D.; Magaña-Aquino, M.; Sánchez-Sánchez, R.; Martinez-Gutierrez, F. Green, Novel, and One-Step Synthesis of Silver Oxide Nanoparticles: Antimicrobial Activity, Synergism with Antibiotics, and Cytotoxic Studies. *New J. Chem.* **2022**, *46*, 17841–17853. [CrossRef]
34. Muthukumar, H.; Palanirajan, S.K.; Shanmugam, M.K.; Arivalagan, P.; Gummadi, S.N. Photocatalytic Degradation of Caffeine and E. Coli Inactivation Using Silver Oxide Nanoparticles Obtained by a Facile Green Co-Reduction Method. *Clean Technol. Environ. Policy* **2021**, *24*, 1087–1098. [CrossRef]
35. Xiao, G.; Zhang, X.; Zhang, W.; Zhang, S.; Su, H.; Tan, T. Visible-Light-Mediated Synergistic Photocatalytic Antimicrobial Effects and Mechanism of Ag-Nanoparticles@chitosan–TiO_2 Organic–Inorganic Composites for Water Disinfection. *Appl. Catal. B Environ.* **2015**, *170–171*, 255–262. [CrossRef]
36. Jiang, Y.; Liu, D.; Cho, M.; Lee, S.S.; Zhang, F.; Biswas, P.; Fortner, J.D. In Situ Photocatalytic Synthesis of Ag Nanoparticles (nAg) by Crumpled Graphene Oxide Composite Membranes for Filtration and Disinfection Applications. *Environ. Sci. Technol.* **2016**, *50*, 2514–2521. [CrossRef] [PubMed]
37. Flak, D.; Braun, A.; Mun, B.S.; Park, J.B.; Parlinska-Wojtan, M.; Graule, T.; Rekas, M. Spectroscopic Assessment of the Role of Hydrogen in Surface Defects, in the Electronic Structure and Transport Properties of TiO_2, ZnO and SnO_2 nanoparticles. *Phys. Chem. Chem. Phys.* **2013**, *15*, 1417–1430. [CrossRef]
38. Nascimben Santos, E.; Ágoston, Á.; Kertész, S.; Hodúr, C.; László, Z.; Pap, Z.; Kása, Z.; Alapi, T.; Krishnan, S.A.G.; Arthanareeswaran, G.; et al. Investigation of the Applicability of TiO_2, $BiVO_4$, and WO_3 Nanomaterials for Advanced Photocatalytic Membranes Used for Oil-in-water Emulsion Separation. *Asia-Pac. J. Chem. Eng.* **2020**, *15*, e2549. [CrossRef]
39. Tansel, B.; Bao, W.Y.; Tansel, I.N. Characterization of Fouling Kinetics in Ultrafiltration Systems by Resistances in Series Model. *Desalination* **2000**, *129*, 7–14. [CrossRef]
40. Li, N.N.; Fane, A.G.; Ho, W.S.W.; Matsuura, T. *Advanced Membrane Technology and Applications*; John Wiley & Sons: Hoboken, NJ, USA, 2011; ISBN 9781118211540.
41. Xie, W.; Li, Y.; Sun, W.; Huang, J.; Xie, H.; Zhao, X. Surface Modification of ZnO with Ag Improves Its Photocatalytic Efficiency and Photostability. *J. Photochem. Photobiol. A Chem.* **2010**, *216*, 149–155. [CrossRef]
42. Liu, S.X.; Qu, Z.P.; Han, X.W.; Sun, C.L. A Mechanism for Enhanced Photocatalytic Activity of Silver-Loaded Titanium Dioxide. *Catal. Today* **2004**, *93–95*, 877–884. [CrossRef]
43. Rebelo, R.; Manninen, N.K.; Fialho, L.; Henriques, M.; Carvalho, S. Morphology and Oxygen Incorporation Effect on Antimicrobial Activity of Silver Thin Films. *Appl. Surf. Sci.* **2016**, *371*, 1–8. [CrossRef]
44. Rafieerad, A.R.; Bushroa, A.R.; Nasiri-Tabrizi, B.; Vadivelu, J.; Basirun, W.J. Silver/Silver Oxide Nanorod Arrays from Physical Vapor Deposition and Subsequent Anodization Processes. *Surf. Coat. Technol.* **2016**, *302*, 275–283. [CrossRef]
45. Mirzaeian, M.; Ogwu, A.A.; Jirandehi, H.F.; Aidarova, S.; Ospanova, Z.; Tsendzughul, N. Surface Characteristics of Silver Oxide Thin Film Electrodes for Supercapacitor Applications. *Colloids Surf. A Physicochem. Eng. Asp.* **2017**, *519*, 223–230. [CrossRef]
46. Restrepo, C.V.; Villa, C.C. Synthesis of Silver Nanoparticles, Influence of Capping Agents, and Dependence on Size and Shape: A Review. *Environ. Nanotechnol. Monit. Manag.* **2021**, *15*, 100428. [CrossRef]
47. Noriega-Treviño, M.E.; Quintero-González, C.C.; Morales-Sánchez, J.E.; Guajardo-Pacheco, J.M.; Compeán-Jasso, M.E.; Ruiz, F. Aggregation Study of Ag-TiO_2 Composites. *Mater. Sci. Appl.* **2011**, *2*, 1719–1723. [CrossRef]

48. Torres-Mendieta, R.; Yalcinkaya, F.; Boyraz, E.; Havelka, O.; Wacławek, S.; Maryška, J.; Černík, M.; Bryjak, M. PVDF Nano-fibrous Membranes Modified via Laser-Synthesized Ag Nanoparticles for a Cleaner Oily Water Separation. *Appl. Surf. Sci.* **2020**, *526*, 146575. [CrossRef]
49. Chen, Q.; Yu, Z.; Li, F.; Yang, Y.; Pan, Y.; Peng, Y.; Yang, X.; Zeng, G. A Novel Photocatalytic Membrane Decorated with RGO-Ag-TiO_2 for Dye Degradation and Oil–Water Emulsion Separation. *J. Chem. Technol. Biotechnol.* **2017**, *93*, 761–775. [CrossRef]
50. Qian, D.; Chen, D.; Li, N.; Xu, Q.; Li, H.; He, J.; Lu, J. TiO_2/Sulfonated Graphene Oxide/Ag Nanoparticle Membrane: In Situ Separation and Photodegradation of Oil/Water Emulsions. *J. Membr. Sci.* **2018**, *554*, 16–25. [CrossRef]
51. Avornyo, A.; Thanigaivelan, A.; Krishnamoorthy, R.; Hassan, S.W.; Banat, F. Ag-CuO-Decorated Ceramic Membranes for Effective Treatment of Oily Wastewater. *Membranes* **2023**, *13*, 176. [CrossRef]